JOURNAL OF AIRCRAFT
Vol. 32, No. 2, March–April 1995

Finite State Induced Flow Models Part I: Two-Dimensional Thin Airfoil

David A. Peters*
Washington University, St. Louis, Missouri 63130
Swaminathan Karunamoorthy†
St. Louis University, Cahokia, Illinois 62206
and
Wen-Ming Cao‡
Washington University, St. Louis, Missouri 63130

A new finite state aerodynamic theory is presented for incompressible, two-dimensional flow around thin airfoils. The theory is derived directly from potential flow theory with no assumptions on the time history of airfoil motions. The aerodynamic states are the coefficients of a set of induced-flow expansions. As a result, the finite state equations are hierarchical in nature and have closed-form coefficients. Therefore, the model can be taken to as many states as are dictated by the spatial texture and frequency range of interest with no intermediate numerical analysis. The set of first-order state equations is easily coupled with structure and control equations and can be exercised in the frequency or Laplace domain as well as in the time domain. Comparisons are given with Theodorsen theory, Wagner theory, and other methods. Excellent results are found with only a few states.

Nomenclature

$[A]$ = matrix of acceleration coefficients, Eq. (35)
$[B]$ = eigenvectors of $[A]$
b = semichord, m
b_n = coefficients of expansion, Appendix C
$C(k)$ = Theodorsen function
c_n = vector of length N, Eq. (31)
D_{nm} = matrix, Eq. (30)
d_n = vector of length N, Eq. (31)
$f(x)$ = generic function $f(x) = g(\eta)$
$g(\eta)$ = generic function
I = identity matrix
j = index taken as s, a, n
k = reduced frequency
$\bar{L}$ = lift per unit length divided by $2\pi\rho bV^2$
$\bar{M}$ = pitching moment about midchord over $2\pi\rho b^2V^2$
$\bar{M}_{1/4}$ = normalized moment about quarterchord
m = index 1, . . . , N
N = number of inflow states
n = index 1, . . . , N
P_p = pressure differential on airfoil, nondimensional on ρV^2
$Q[f]$ = functional, Eq. (18)
s = Laplace variable
T_n = eigenvalues of $[A]$
t = reduced time, normalized on semichord and freestream
u = x component of induced velocity, normalized on V
V = freestream velocity, m/s
v = y component of induced velocity, normalized on V
$W(t)$ = Wagner function
w = total induced downwash, $-v$
w_j = coefficients of w expansion, Eq. (22)
x, y = Cartesian coordinates normalized on b
$Y(Z)$ = weighting function
Z = wake variable, $e^{-\eta}$
Γ = total bound vorticity divided by bV
$\bar{\Gamma}$ = normalized vorticity, $\Gamma/2\pi$
γ = vorticity density divided by V
γ_b = bound vorticity density
γ_j = expansion coefficients of vorticity and velocity, Eqs. (11) and (12)
γ_w = wake vorticity density
Δ = elliptical determinant, Appendix A
∇ = Laplace operator
$\delta(t)$ = impulse function
ε = residual error, Eq. (43)
λ = induced flow due to shed vorticity divided by V
λ_j = expansion terms for λ, Eq. (17)
$\bar{\lambda}_j$ = complex representation of λ_j
ξ = streamwise direction
ρ = density of air, kg/m^3
τ_j = pressure expansion coefficients, Eqs. (13) and (14)
Φ_j = acceleration potentials, Appendix A
Ψ_j = velocity potentials, Appendix A

Superscripts
A = from acceleration term
T = transpose
V = from velocity term
$'$ = $-\partial/\partial y$
$\cdot$ = $\partial/\partial t$
$\hat{}$ = evaluated on upper surface of airfoil

Subscripts
a = asymmetric potential
L = lower surface
s = symmetric potential
U = upper surface

Received Sept. 13, 1993; revision received May 23, 1994; accepted for publication June 17, 1994.

*Professor and Director, Center for Computational Mechanics, Campus Box 1129. Fellow AIAA.
†Associate Professor, Department of Aerospace Engineering, Parks College. Member AIAA.
‡Graduate Research Assistant, Department of Mechanical Engineering, Campus Box 1185.

Introduction

Background

UNSTEADY aerodynamic models that are useful for aeroelastic analysis are usually of four general types. First, there are k-type aerodynamic theories in which the motions, pressure, and induced flow undergo only simple harmonic motion, e^{ikt}. These are often used in the V-g method but, strictly-speaking, they are accurate only at the stability boundary. A second category of model has p-type (or Laplace-domain) aerodynamics in which the aerodynamic variables undergo exponentially growing (or decaying) harmonic motion. This type of model is utilized in eigenanalysis in which an iteration on p (i.e., on s) is performed for every eigenvalue of interest. A third type of aerodynamic model is indicial, in which a Green's function is utilized with a convolution integral to give arbitrary motion response. This is useful in time-marching. In principle, these three types of aerodynamics are equivalent and can be derived from one another through Laplace and Fourier transforms.

A fourth type of unsteady aerodynamics is the class of finite state models. In a precise sense, two-dimensional unsteady aerodynamics has no finite state representation, but is an infinite state process [e.g., $s\sqrt{s}$ terms appear in the transfer function]. Nevertheless, useful finite state approximations have been derived. There are several advantages of finite state models. First, finite state modeling allows one to cast the aerodynamics in the same state-space context as the structural dynamics and controls. This allows the full complement of control theory and systems theory to be brought to bear on the problem of aero-servo-elastic control and design. Second, the existence of explicit states eliminates the necessity to iterate on solutions (as in V-g and p-k methods). Instead, the entire solution can be obtained in one pass. Third, a state-space model is flexible in that it can be exercised in the frequency domain, Laplace domain, or the time domain as desired.

There are several types of finite state models. Vortex-lattice and computational fluid dynamics (CFD) methods can be cast as finite state models with the number of states being the order of the number of lattice nodes or CFD grid points. This, however, is usually such a large number of states that conventional control-theory applications are precluded. Instead, most applications of finite state models to aeroelasticity have utilized a relatively few approximate states. The disadvantages of this are that such states have no direct physical interpretation and that they cannot be systematically improved in a hierarchical manner. It would seem, therefore, useful to have a more general finite state model.

Previous Work

In 1925, Wagner published the indicial function for the lift response of a two-dimensional, flat-plate airfoil in incompressible flow.[1] In 1935, Theodorsen presented the lift frequency response for the same conditions.[2] Garrick then showed that the two were related (and mutually consistent) by means of Fourier transform.[3] The use of Laplace transform (p-version aerodynamics) was suggested by Jones,[4] and applied to some problems by Sears.[5] Jones[4] obtained an approximate Laplace transform of the Wagner function,[6] but Jones[7] was the first to generalize the Theodorsen function formally for p-type motions. At that time, the major mathematical concern was whether or not this generalization was applicable for decaying motion (negative real part of s).[8] This skepticism prevailed despite the arguments from analytic continuation.[9] Thus, work on time domain unsteady aerodynamics was at a standstill.

Some 25 years later, interest was renewed in time-domain methods. Hassig[10] used rational functions in the Laplace domain. Vepa[11] introduced the method of Padé approximants to give a finite state representation of any aerodynamic frequency-domain lift function,[11] as did Dowell.[12] The authors of Refs. 13 and 14 attacked the problem for two-dimensional compressible and incompressible flows. Their work is in the Laplace domain and builds on the work of Sears.[5] It utilizes numerical methods to locate the poles and to perform the inverse Laplace transform by contour integration.[13,14] Work further developed for the three-dimensional case (finite wing),[15,16] but that is the subject of Part II, the sequel to this article.

In rotorcraft aeroelasticity, the development of time-domain (rather than frequency-domain) unsteady aerodynamics is particularly crucial due to the existence of periodic coefficients and nonlinear stall, which preclude superposition of Fourier or Laplace solutions. The fundamental frequency-domain result was derived by Loewy.[17] It is an extension of the Theodorsen theory and assumes layers of vorticity below the airfoil to account for the returning wake. However, its application is limited to linear problems of hover and climb. Dinyavari and Friedmann[18] used Padé approximants of both Theodorsen and Loewy functions in order to accommodate some unsteady aerodynamics into periodic-coefficient Floquet stability analysis. Most dynamic stall models for rotorcraft (e.g., Ref. 19) utilize the Wagner function in a convolution integral to account for the time variation in induced flow due to the vorticity shed from stall. One exception is the ONERA dynamic stall model,[20] in which a first-order differential equation provides a single-state approximation to the Theodorsen function. (This is in contrast to the normal two-state approximations, Refs. 8 and 18.) In Ref. 21, the ONERA model is generalized as a vorticity-based model, but still with a one-state Theodorsen model. In Ref. 22, the one-state model is replaced by a hierarchical finite state inflow model for rotors.

Present Approach

In this article we offer a new type of finite state aerodynamic model. The model offers finite state equations for the induced flowfield itself. These equations are derived directly from the potential flow equations (either velocity or acceleration potential). Thus, no intermediate steps are invoked in which restrictions are placed on blade motions; and the theory is an arbitrary-motion theory from the outset. In contrast to CFD and vortex lattice methods, the states represent induced flow expansion fields rather than velocities at discrete nodes. As a result, the states are hierarchical, and the equation coefficients are known in closed form. No numerical fitting of frequency-response or indicial functions is needed.

Furthermore, the induced-flow expansion implies that only a few states are needed, and the number of states can be chosen a priori based either on the texture required in the induced flowfield or on the frequency range of interest. The resultant equations are easily coupled with structural or control equations and can be exercised in the frequency-domain, Laplace domain, or time domain.

The above approach can be followed either in two- or three-dimensional flow. In this article, Part I, we consider two-dimensional flow about a finite strip (i.e., airfoil) and apply the nonpenetration condition to recover thin airfoil theory. In the sequel, Part II, we will apply the approach to the three-dimensional flow about a disk (i.e., rotor). The disk is taken as penetrable (an actuator disc) for application to rotorcraft rather than circular wings. For flow near the blades, Part II utilizes the lift equation of Part I, but with the three-dimensional induced-flow model. Thus, this article forms a basis for rotor inflow as well as for two-dimensional aerodynamics.

Theoretical Background

Fluid Mechanics

The airfoil lies on the segment $y = 0$, $-1 < x < +1$ in the nondimensional coordinate system of Appendix A. If we define u and v as the nondimensional x and y velocity com-

ponents, and if we assume the freestream velocity (normalized to unity) is in the ξ direction, then the continuity and momentum equations are

$$\frac{\partial u}{\partial x} + \frac{\partial v}{\partial y} = 0$$

$$\frac{\partial u}{\partial t} + \frac{\partial u}{\partial \xi} = \frac{-\partial \Phi}{\partial x}$$

$$\frac{\partial v}{\partial t} + \frac{\partial v}{\partial \xi} = \frac{-\partial \Phi}{\partial y} \tag{1}$$

We then define special potential functions Φ^V and Φ^A:

$$\frac{\partial \Phi^A}{\partial x} \equiv \frac{-\partial u}{\partial t}, \qquad \frac{\partial \Phi^A}{\partial y} \equiv \frac{-\partial v}{\partial t}$$

$$\frac{\partial \Phi^V}{\partial x} \equiv \frac{-\partial u}{\partial \xi}, \qquad \frac{\partial \Phi^V}{\partial y} \equiv \frac{-\partial v}{\partial \xi} \tag{2}$$

The continuity and momentum equations are then fulfilled if Φ^A and Φ^V satisfy

$$\Phi^V + \Phi^A = \Phi \tag{3a}$$

$$\nabla^2 \Phi^V = \nabla^2 \Phi^A = \nabla^2 \Phi = 0 \tag{3b}$$

The velocity field may be found from Φ^V by

$$u = -\int_{-\infty}^{\xi} \frac{\partial \Phi^V}{\partial x}\, d\bar{\xi}, \qquad v = -\int_{-\infty}^{\xi} \frac{\partial \Phi^V}{\partial y}\, d\bar{\xi} \tag{4}$$

The only pressure discontinuity allowed is across the airfoil, and specification of the time history of this discontinuity defines the pressures and velocities everywhere.

For the case of edgewise flow ($\xi = x$), we have

$$u = -\Phi^V, \quad \Phi^V = \int_{-\infty}^{t} \frac{\partial \Phi^A}{\partial x}\, d\bar{t}, \quad \Phi^A = \int_{-\infty}^{x} \frac{\partial \Phi^V}{\partial t}\, d\bar{x} \tag{5}$$

$$\Phi = \Phi^A + \frac{\partial}{\partial x} \int_{-\infty}^{t} \Phi^A\, d\bar{t}$$

$$\Phi = \Phi^V + \frac{\partial}{\partial t} \int_{-\infty}^{x} \Phi^V\, d\bar{x} \tag{6}$$

It follows that there is a strip of concentrated vorticity γ that exists on $y = 0$, $-1 \le x < \infty$. On the airfoil ($-1 < x < +1$) it is the bound vorticity γ_b; and behind the airfoil ($1 < x < \infty$) it is the wake vorticity γ_w. From the definition of vorticity and the integration around a small loop across this strip, one can relate γ, Φ^V, and P_D (the pressure across the vorticity sheet):

$$\gamma = \Phi^V_L - \Phi^V_U, \qquad P_D = \Phi_L - \Phi_U \tag{7}$$

From Eq. (6b) we then have the pressure-vorticity relation

$$P_D = \gamma_b + \frac{\partial}{\partial t} \int_{-1}^{x} \gamma_b\, d\bar{x} \tag{8a}$$

$$0 = \gamma_w + \dot{\Gamma} + \frac{\partial}{\partial t} \int_{1}^{x} \gamma_w\, d\bar{x} \tag{8b}$$

$$\Gamma = \int_{-1}^{+1} \gamma_b\, dx = -\int_{+1}^{\infty} \gamma_w\, dx \tag{9}$$

(with zero initial conditions). It follows that

$$\frac{\partial P_D}{\partial x} = \frac{\partial \gamma_b}{\partial x} + \frac{\partial \gamma_b}{\partial t} \tag{10a}$$

$$0 = \frac{\partial \gamma_w}{\partial x} + \frac{\partial \gamma_w}{\partial t} \tag{10b}$$

$$\gamma_w(x, t) = -\dot{\Gamma}(t - x + 1) \tag{10c}$$

Clearly, the velocity u is discontinuous across the vortex sheet; but the normal velocity v is continuous. Thus, Φ^V is discontinuous, but $\partial \Phi^V / \partial x$ is continuous.

Equations for Bound Vorticity

In order to obtain a set of state-variable equations for the induced flow, we can treat the circulation-based equations in the previous section with an expansion. To begin, we consider the induced flow due only to γ_b. This induced flow is independent of the time history of γ_b. Thus, due to the asymmetry about $y = 0$, we can write Φ^V (and γ_b) as expansions in the potential functions of Appendix A

$$\Phi^V = -\sum_j \gamma_j \Phi_j, \qquad \gamma_b = 2 \sum_j \gamma_j \hat{\Phi}_j \tag{11}$$

where j takes on the values $s, a, 1, 2, 3, 4, \ldots$, and $\hat{}$ implies evaluation on the upper surface. The velocity field from this bound vorticity then follows either from the Biot-Savart law,[23] or from Eq. (4b):

$$-v = \text{downwash} = \sum_j \gamma_j \Psi'_j \tag{12}$$

Thus, the γ_j represents both bound vorticity coefficients and downwash coefficients, which are exactly the Glauert velocity expansions.

Returning to the dynamic case, we see that these downwash coefficients can be related to the airfoil differential pressure by Eq. (8a). Thus, if we expand the pressure in a series similar to that for vorticity

$$\Phi = -\sum_j \tau_j \Phi_j, \qquad P_D = 2 \sum_j \tau_j \hat{\Phi}_j \tag{13}$$

then we obtain from Eq. (8a)

$$\sum_j \tau_j \hat{\Phi}_j = \sum_j \gamma_j \hat{\Phi}_j + \sum_j \dot{\gamma}_j \hat{\Psi}_j \tag{14}$$

However, from Appendix A we see that the $\hat{\Psi}_j$ can be uniquely expressed in terms of the $\hat{\Phi}_j$. This allows a balancing of coefficients in Eq. (14), since the $\hat{\Phi}_j$ are linearly independent. The result of this balancing is a set of ordinary differential equations that relate the velocity coefficients γ_j and the pressure coefficients τ_j.

$$\gamma_s = \tau_s, \qquad \gamma_a = \tau_a \tag{15a}$$

$$\dot{\gamma}_a - \tfrac{1}{2}\dot{\gamma}_2 + \gamma_1 = \tau_1 - 2\dot{\bar{\Gamma}} \tag{15b}$$

$$(1/2n)(\dot{\gamma}_{n-1} - \dot{\gamma}_{n+1}) + \gamma_n = \tau_n - (2/n)\dot{\bar{\Gamma}}$$

$$n = 2, 3, 4, \ldots \tag{15c}$$

where $\bar{\Gamma}$ is the normalized total bound vorticity

$$\bar{\Gamma} \equiv \Gamma/2\pi = \gamma_s + \tfrac{1}{2}\gamma_1 \tag{16}$$

Wake Vorticity

The next step in the derivation is to find equations for the induced flow due to shed wake vorticity λ. From Ref. 23, we

see that this component of downwash can be expanded (on the airfoil) in a similar fashion as w, Eq. (12)

$$\lambda = \sum_j \lambda_j \hat{\Psi}'_j \qquad j \neq s \tag{17}$$

where $\lambda_a = \lambda_0$ of Ref. 21 and λ_s is not used since $\Psi'_s = 0$ on $-1 < x < +1$. Reference 23 provides formulas for λ_j in terms of the wake vorticity. For simplicity, we write these as functionals:

$$Q[f(x)] \equiv -\frac{1}{\pi}\int_1^\infty \gamma_w f(x)\,dx = -\frac{1}{\pi}\int_0^\infty \gamma_w g(\eta)\sinh(\eta)\,d\eta$$

$$\bar{\Gamma} = \frac{1}{2}Q[1]$$

$$\lambda_a = \frac{1}{2}Q\left[\frac{1}{\sinh(\eta)}\right] = \frac{1}{2}Q[\Psi'_s]$$

$$\lambda_n = Q\left[\frac{e^{-n\eta}}{\sinh(\eta)}\right] = Q\left[-\frac{1}{n}\Phi'_n\right] \tag{18}$$

We note that the above formulas imply that a differential equation for this functional can be obtained based on Eq. (10c) and integration by parts

$$\dot{Q}[f] = \frac{1}{\pi}\int_1^\infty \frac{d\gamma_w}{dx} f(x)\,dx$$

$$\dot{Q}[f] = -\frac{1}{\pi}f(1)\gamma_w(1) - \frac{1}{\pi}\int_1^\infty \gamma_w \frac{df}{dx}\,dx$$

$$\dot{Q}[f] = 2\dot{\bar{\Gamma}}f(1) + Q\left[\frac{df}{dx}\right]$$

$$\dot{Q}[f] = 2\dot{\bar{\Gamma}}g(0) + Q\left[\frac{dg/d\eta}{\sinh(\eta)}\right] \tag{19}$$

When Eq. (19) is applied to the λ_j functionals in Eq. (18), one must insure that $g(0) = f(1)$ is finite. Therefore, we use $\dot{\lambda}_{n-1} - \dot{\lambda}_{n+1}$ as the left side of Eq. (8), which gives a $g(\eta)$ of the form:

$$g(\eta) = [e^{-(n-1)\eta} - e^{-(n+1)\eta}]/\sinh\eta = 2e^{-n\eta} \tag{20}$$

The resultant differential equations are

$$\dot{\lambda}_a - \tfrac{1}{2}\dot{\lambda}_2 + \lambda_1 = 2\dot{\bar{\Gamma}}$$

$$(1/2n)(\dot{\lambda}_{n-1} - \dot{\lambda}_{n+1}) + \lambda_n = (2/n)\dot{\bar{\Gamma}} \qquad n = 2, 3, 4\ldots \tag{21}$$

The similarity with the γ_j equations [Eqs. (15)], is striking.

Boundary Conditions

It is especially interesting to use Eqs. (15) and (21) to form differential equations for the total induced flow w (downwash due to bound plus wake vorticity). If we expand w as

$$w = \sum_j w_j \hat{\Psi}'_j, \qquad j \neq s$$

$$w_j = \gamma_j + \lambda_j, \qquad j \neq s \tag{22}$$

then, by addition of Eq. (15) and (21), we have

$$w_a - \lambda_a = \tau_a$$

$$\dot{w}_a - \tfrac{1}{2}\dot{w}_2 + w_1 = \tau_1$$

$$(1/2n)(\dot{w}_{n-1} - \dot{w}_{n+1}) + w_n = \tau_n \tag{23}$$

These equations can also be obtained from a direct application of the acceleration potential, Appendix B and Ref. 24.

It is important to note in Eq. (23) that w (the total downwash) is completely determined by the nonpenetration boundary condition. Thus, for small airfoil deformations $y(x, t)$, $-1 < x < +1$

$$w = -\left(\frac{\partial y}{\partial x} + \frac{\partial y}{\partial t}\right) \tag{24}$$

Therefore, the only unknown in the entire airfoil loading (τ_j) is λ_a. Of particular interest are the normalized lift $\bar{L}$, the normalized pitching moment about midchord $\bar{M}$, and the moment about the quarterchord $\bar{M}_{1/4}$:

$$\bar{L} = \tau_s + \tfrac{1}{2}\tau_1$$

$$\bar{M} = \tfrac{1}{2}\tau_a - \tfrac{1}{4}\tau_2$$

$$\bar{M}_{1/4} = \bar{M} - \tfrac{1}{2}\bar{L} \tag{25}$$

From Eqs. (23) and the Kutta condition ($\tau_s = \tau_a = \gamma_s = \gamma_a$), we then can write

$$\bar{L} = w_a + \tfrac{1}{2}w_1 - \lambda_a + \tfrac{1}{2}(\dot{w}_a - \tfrac{1}{2}\dot{w}_2) \tag{26a}$$

$$\bar{M} = \tfrac{1}{2}(w_a - \lambda_a) - \tfrac{1}{4}w_2 - \tfrac{1}{16}(\dot{w}_1 - \dot{w}_3) \tag{26b}$$

$$\bar{M}_{1/4} = -\tfrac{1}{4}(w_1 + w_2) - \tfrac{1}{4}(\dot{w}_a - \tfrac{1}{2}\dot{w}_2) - \tfrac{1}{16}(\dot{w}_1 - \dot{w}_3) \tag{26c}$$

Historically, $w_a + \frac{1}{2}w_1$ has been called the quasisteady lift, $w_a + \frac{1}{2}w_1 - \lambda_a$ the circulatory lift, and $\frac{1}{2}(\dot{w}_a - \frac{1}{2}\dot{w}_2)$ the noncirculatory lift. Since $\bar{M}_{1/4}$ (and all higher pressure coefficients τ_n) are completely determined by airfoil motion, we concentrate on $\bar{L}$ and λ_a for the remainder of this article. The power of Eq. (26a) for $\bar{L}$ in terms of λ_a is that the λ_n solution does not need to have the fidelity necessary to meet explicit boundary conditions. We need only an accurate λ_a.

Equation (21) gives relationships for the λ_n. Unfortunately, λ_a cannot be determined from Eq. (21) alone. One additional relation is needed that relates λ_a to the λ_n. From the operator notation in Eq. (18) and the shorthand notation $Z = e^{-\eta}$, we see that if one could approximate unity on $0 \leq \eta < \infty$ by

$$1 \approx \sum_{n=1}^{N} b_n Z^n \qquad 0 < Z \leq 1 \tag{27}$$

then one could approximate λ_a by

$$\lambda_a \approx \frac{1}{2}\sum_{n=1}^{N} b_n \lambda_n \tag{28}$$

Although Eq. (27) can never hold at $Z = 0$, the approximation must converge only on the open interval (excluding $Z \equiv 0$ at $\eta \to \infty$). Thus, unity can be represented as a power series. Closed-form results for the b_n are given in Appendix C. The result is a set of finite state equations for the λ_n and (more importantly) for λ_a. The equations are comprised of Eqs. (21) and (28) with

$$\bar{\Gamma} = \gamma_a + \tfrac{1}{2}\gamma_1 = w_a - \lambda_a + \tfrac{1}{2}(w_1 - \lambda_1) \tag{29}$$

These, along with Eqs. (26), form a finite state theory of unsteady aerodynamics in which the states are the Glauert inflow distributions.

Application

Matrix Form

In order to verify the finite state aerodynamic model given by Eqs. (21), (26a–26c), (28), and (29), we apply it to the cases of the Theodorsen and Wagner functions. To facilitate this application, the theory is put into matrix form. First, we

define the following matrices (in addition to the expansion coefficients b_n, Appendix C):

$$D_{nm} = \tfrac{1}{2}n \qquad (n = m + 1)$$
$$D_{nm} = -\tfrac{1}{2}n \qquad (n = m - 1)$$
$$D_{nm} = 0 \qquad n \neq m \pm 1 \tag{30}$$

$$d_n = \tfrac{1}{2} \qquad n = 1$$
$$d_n = 0 \qquad n \neq 1$$
$$c_n = 2/n \tag{31}$$

Then we rewrite Eq. (21) as

$$[D + \mathrm{d}b^T]\{\dot{\lambda}\} + \{\lambda\} = \{c\}\dot{\bar{\Gamma}} \tag{32}$$

where

$$\lambda_a = \tfrac{1}{2}b^T\lambda_n$$
$$\bar{\Gamma} = (w_a + \tfrac{1}{2}w_1) - (\lambda_a + \tfrac{1}{2}\lambda_1)$$
$$\bar{L} = w_a + \tfrac{1}{2}w_1 - \lambda_a + \tfrac{1}{2}(\dot{w}_a - \tfrac{1}{2}\dot{w}_2) \tag{33}$$

Alternately, we may write

$$[A]\{\dot{\lambda}\} + \{\lambda\} = \{c\}(\dot{w}_a + \tfrac{1}{2}\dot{w}_1) \tag{34}$$

where

$$[A] = [D + \mathrm{d}b^T + c\,\mathrm{d}^T + \tfrac{1}{2}cb^T] \tag{35}$$

Special Cases

The Theodorsen function is defined as the ratio of circulatory lift to quasisteady lift (in the complex domain) for motion of the form e^{ikt}. Thus

$$C(k) = \frac{w_a + \tfrac{1}{2}w_1 - \lambda_a}{w_a + \tfrac{1}{2}w_1} = \frac{\bar{\Gamma} + \tfrac{1}{2}\lambda_1}{\bar{\Gamma} + \lambda_a + \tfrac{1}{2}\lambda} \tag{36}$$

For $\lambda_n = \bar{\lambda}_n e^{ikt}$, $\bar{\Gamma} = e^{ikt}$, we have

$$C(k) = \frac{1 + \tfrac{1}{2}\bar{\lambda}_1}{1 + \bar{\lambda}_a + \tfrac{1}{2}\bar{\lambda}_1}$$
$$\{\bar{\lambda}\} = [(D + \mathrm{d}b^T)ik + I]^{-1}\{c\}ik$$
$$\bar{\lambda}_a = \tfrac{1}{2}b^T\bar{\lambda}_n, \qquad \tfrac{1}{2}\bar{\lambda}_1 = \mathrm{d}^T\lambda \tag{37}$$

Equation (37) defines the Theodorsen function for any N. It is interesting to contrast the simplicity of form of Eq. (37) with the complexity of the Bessel functions in Theodorsen theory.

The Wagner function is defined as the circulatory lift $w_a + \tfrac{1}{2}w_1 - \lambda_a$, for the special case $w_a = u(t)$, step function, and $w_1 = 0$. From Eq. (26), this reduces to

$$W(t) = 1 - \lambda_a(t) = 1 - \sum_{n=1}^{N} \frac{1}{2} b_n\lambda_n(t) \tag{38}$$

where $\lambda_n(t)$ is the solution to Eqs. (34), i.e.,

$$[A]\{\dot{\lambda}\} + \{\lambda\} = \{c\}\delta(t), \quad \{\lambda(0)\} = (0) \tag{39}$$

or

$$[A]\{\dot{\lambda}\} + \{\lambda\} = \{0\}, \quad \{\lambda(0)\} = [A]^{-1}\{c\} \tag{40}$$

Equation (40) can be solved by time-marching or by utilization of the eigenvalues and eigenvectors of $[A]$, T_n, and B. (T_n are time constants of the flow.)

$$[B]^{-1}[A][B] = [T_n]$$
$$\{\lambda(t)\} = [B][e^{-t/T_n}][B]^{-1}[A]^{-1}\{c\}$$
$$= [B][e^{-t/T_n}/T_n][B]^{-1}\{c\} \tag{41}$$

The limiting cases of the Theodorsen and Wagner functions are determined by the b_n. An interesting limit is the slope of the imaginary part of $C(k)$ as k approaches zero. Theoretically, as k approaches zero the slope of $C(k)$ goes to infinity like $\ell n(k)$. Interestingly, one can show that the finite state model gives this slope as

$$\lim_{k\to 0} \frac{\partial C(k)}{\partial(ik)} = -\sum_{n=1}^{N} b_n/n \tag{42}$$

Appendix C shows that this sum is an approximation to $\ell n(0)$, and approaches $-\infty$ as N increases.

Another interesting limiting case is the limit of $C(k)$ as k approaches ∞, and the limit of $W(t)$ as t approaches zero. Theoretically, these should be equal to each other and equal to 0.5. Although the algebra is a little involved, one can show that: 1) if $\Sigma\, b_n = 1$ and $\Sigma\, nb_n = 0$ (as in the binomial expansion for b_n, Appendix C), then $C(k)$ and $W(t)$ will equal exactly 0.5 in the finite state model; and 2) if $\Sigma\, b_n = 1$, then $C(k)$ and $W(t)$ will approach 0.5 as N becomes large. For example, for N odd

$$\lim_{k\to\infty} C(k) = W(0) = \frac{1}{2} + \frac{\varepsilon/2}{2 + \varepsilon}$$
$$\varepsilon = \sum_{n=1,2,3,}^{N} nb_n \Big/ \left[(N + 1)\sum_{n=1,3,5}^{N} b_n\right] \tag{43}$$

Since the b_n alternate signs as $(-1)^{n+1}$, $W(0)$ begins at 0.6 for $N = 1$, $b_1 = 1$, and quickly approaches 0.5 as N increases. Lastly, one can show that the sum of all the eigenvalues of $[A]$ equals the trace $[A]$. Thus,

$$\sum_{n=1}^{N} T_n = 1 + \frac{1}{2}b_1 + \sum_{n=1}^{N} b_n/n \tag{44}$$

which also approaches ∞ as N becomes large.

Results

We would now like to examine the convergence of the finite state model for various choices of b_n. Figure 1 compares the Re[$C(k)$], Im[$C(k)$], and $W(t)$ with the finite state approximations for $N = 4$. In order to see the performance over the entire range of k or t, the Theodorsen function is plotted vs $k/(1 + k)$, and the Wagner function is plotted vs $t/(2\pi + t)$. Exact solutions are obtained numerically. One can see that the augmented least-squares series for b_n (see Appendix C for closed-form) gives a reasonable fit. The other least-squares methods (not shown in the figure) give a similar result. The binomial expansion, which is designed to give least error at large k (and small t), does so, but to the detriment of small k (or large t) response. Figure 2 shows a similar comparison for $N = 8$. The error is greatly reduced, although the binomial expansion is converging slowly.

Figure 3 presents a quantitative measure of an error norm defined as the rms error computed on 100 equally spaced points on the $k/(1 + k)$ or $t/(2\pi + t)$ plot. The error is normalized such that the $N = 0$ case, $C(k) = W(t) = 1$, has an error of unity. We see that the binomial expansion converges at a rate of N^{-1}, whereas the augmented least squares converges as N^{-2}. However, due to the large factorials in the augmented method, double precision arithmetic fails for $N >$ 10 for $C(k)$ and $N > 8$ for $W(t)$. The minimum error for the augmented least squares occurs at $N = 8$, and is 1% for $C(k)$

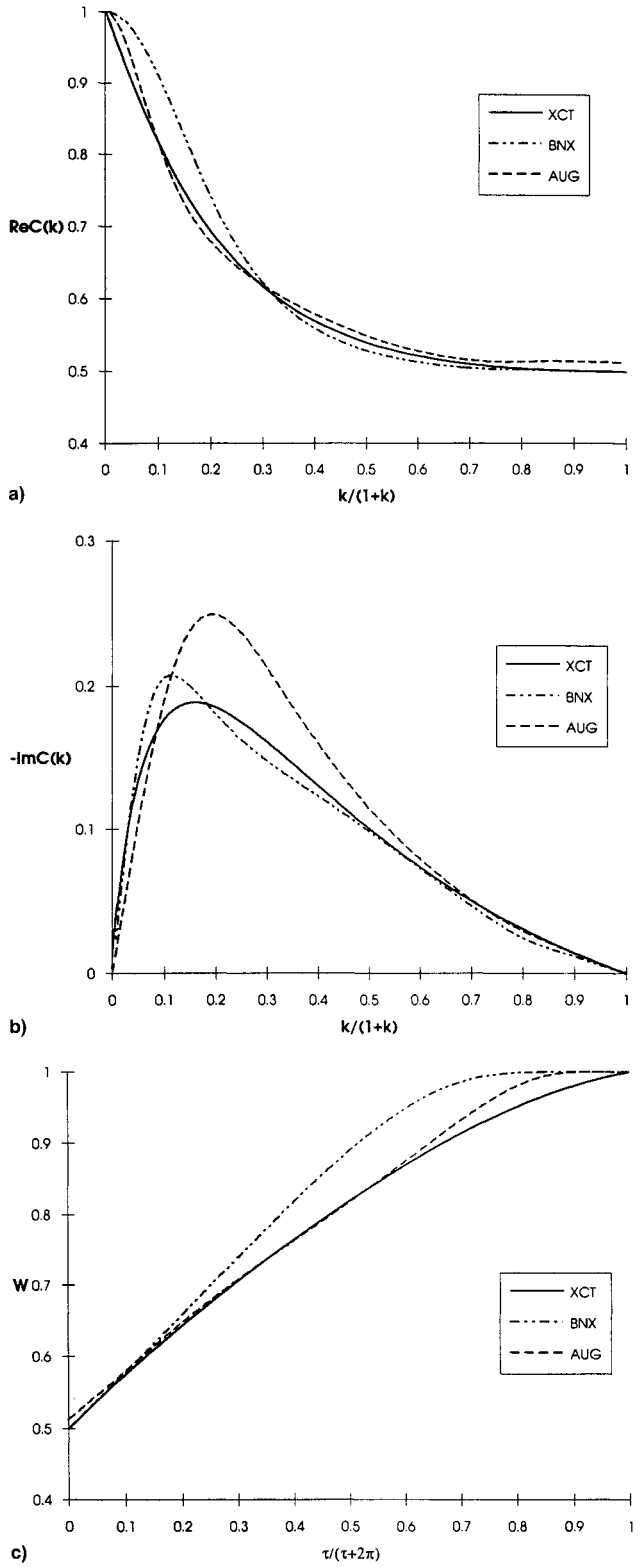

Fig. 1 a) Real part of $C(k)$, $N = 4$; b) imaginary part of $C(k)$, $N = 4$; and c) Wagner function, $N = 4$.

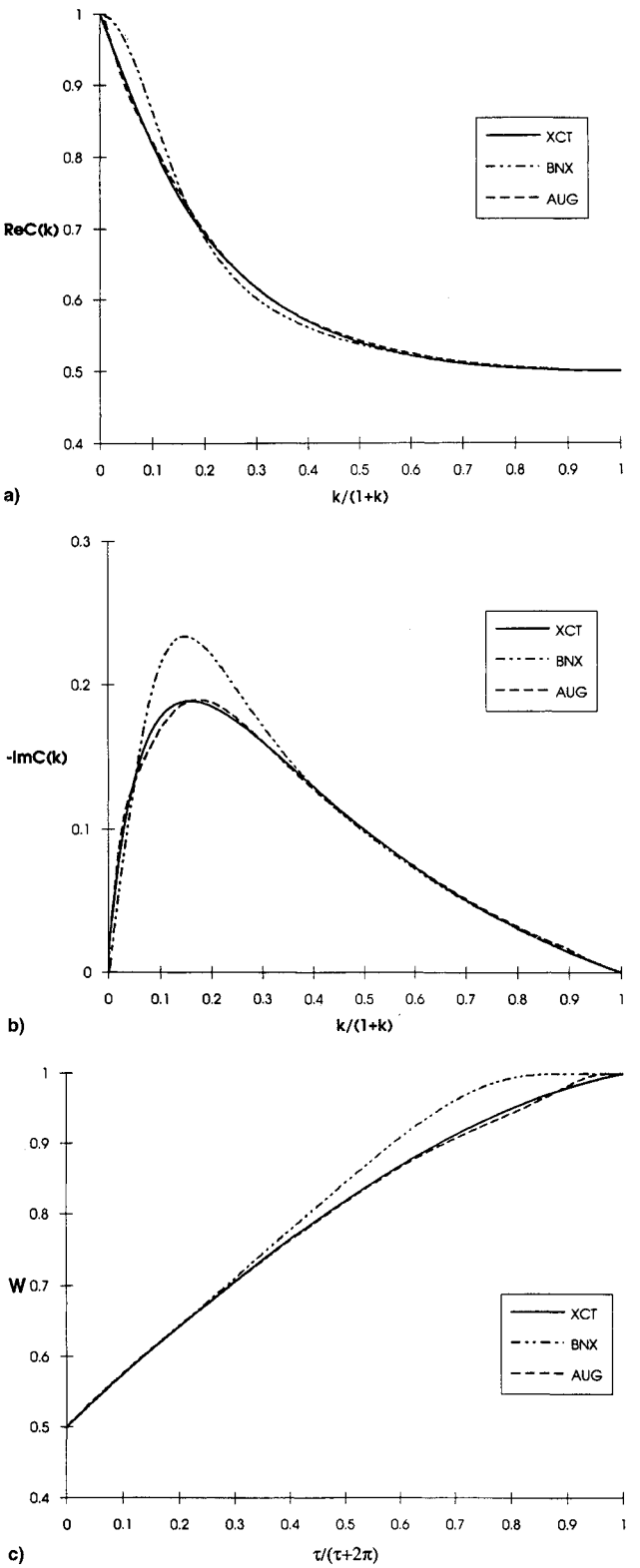

Fig. 2 a) Real part of $C(k)$, $N = 8$; b) imaginary part of $C(k)$, $N = 8$; and c) Wagner function, $N = 8$.

and 1.3% for $W(t)$. The binomial expansion (with smaller factorials than the augmented least squares) begins to diverge after $N = 50$ for $C(k)$ and $N = 16$ for $W(t)$. (Recall that eigenvalue problems are more sensitive than are matrix inversions.) The minimum error is 0.7% for $C(k)$ ($N = 50$) and 5% for $W(t)$ ($N = 16$). Quadruple precision would extend the accuracy of either method.

Table 1 provides a summary of these errors and compares them with those from Jones' approximation (which has two states), and with Padé approximants with two and three states, respectively. Note that the Jones' method, which is based on a fit of the Wagner function, has a lower error norm for $W(t)$ than it does for $C(k)$. Conversely, the Padé results, based on a least-squares fit of $C(k)$, have a lower error norm for $C(k)$ than they do for $W(t)$. It is at first puzzling to see that one needs four to six inflow states with the augmented method to obtain the same accuracies as can be obtained with only two to three states for Jones' and Padé methods. The reason for

Table 1 Error norms

Methods	Theodorsen	Wagner
Curve-fit		
Jones	2.3%	1.8%
Padé, $N = 2$	2.1%	3.8%
Padé, $N = 3$	1.2%	3.4%
Augmented		
$N = 4$	3.5%	5.0%
$N = 6$	1.6%	1.8%
$N = 8$	1.0%	1.3%
Binomial		
$N = 4$	10.5%	18.3%
$N = 8$	5.6%	10.1%
$N = 16$	2.8%	5.0%
$N = 30$	1.3%	—
$N = 50$	0.7%	—

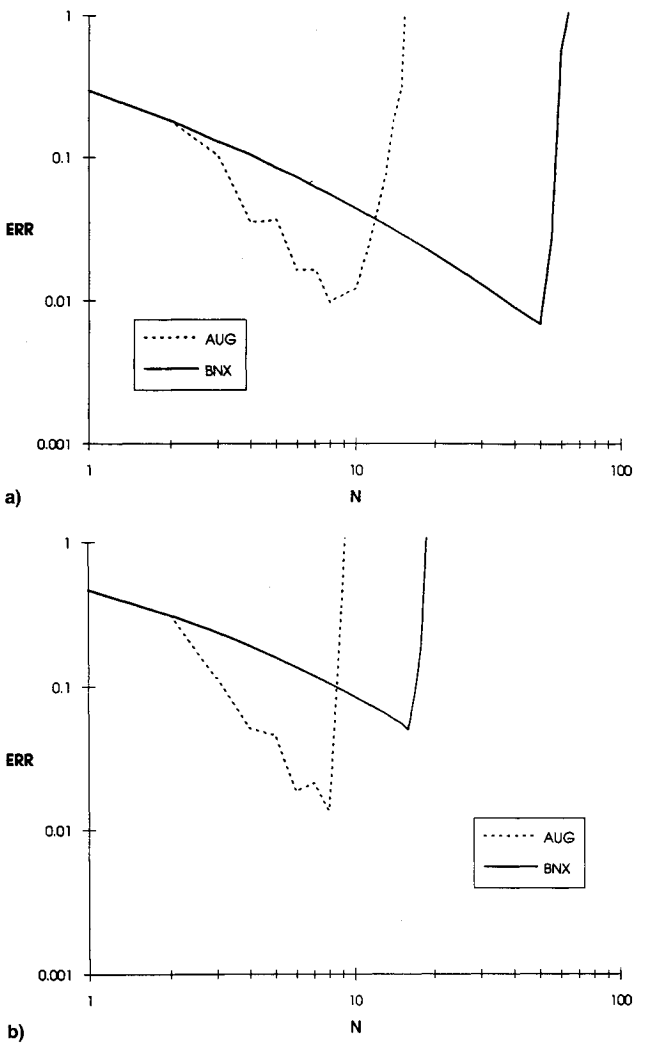

Fig. 3 Error norm for a) $\sqrt{(\text{Re } C)^2 + (\text{Im } C)^2}$ and b) $\sqrt{W^2}$.

this phenomenon is found in a study of the eigenvalues of the system. The accuracy of the finite state model is obtained almost entirely from the first two to three eigenvalues (which are real), even for $N = 50$. Thus, only a few states are required; but they are a combination of many of the Glauert states. One might suspect, therefore, that a change of variable could improve the convergence of the finite state results.

Conclusions

A finite state induced flow model has been developed from first principles (as opposed to numerical fits of Theodorsen or Wagner functions). The method is hierarchical, and the states represent the classical Glauert induced flow coefficients. The resultant, closed-form equations for the inflow and states give excellent correlation with Theodorsen and Wagner functions with four to nine states included. This finite state type of aerodynamic analysis is very useful in aeroelasticity because it can be used in the frequency domain, Laplace domain, or the time domain. Furthermore, the method is more rigorous than other finite state methods in that it is based on first-principle fluid mechanics rather than on curve-fitting specialized response functions; and the method is more computationally direct than methods based on extensions in the complex plain that require extensive numerical analysis.

The weakness of the method is that convergence is not as rapid as is theoretically possible. An appropriate change of variable in the inflow expansion could cure this.

Appendix A: Potential Functions with Elliptical Coordinates

Coordinates

We define an x, y coordinate system with positive x downstream and positive y in the direction of positive lift. All lengths are nondimensional on b, such that the airfoil is on the line segment $-1 < x < +1$, $y = 0$. Pressures are normalized on ρV^2, and time is normalized on the semichord over velocity. (It follows that velocities are normalized on V.) The transformation from elliptical coordinates to Cartesian coordinates is given by

$$x = \cosh \eta \cos \phi, \qquad y = \sinh \eta \sin \phi$$
$$0 \le \phi < 2\pi, \qquad 1 \le \eta < \infty \tag{A1}$$

Thus, upstream $\phi = \pi$, $x = -\cosh \eta$, $y = 0$; downstream $\phi = 0$, $x = \cosh \eta$, $y = 0$; and on the airfoil $\eta = 0$, $x = \cos \phi$, $y = 0$. The transformation of derivatives is given by

$$\begin{Bmatrix} \frac{\partial}{\partial x} \\ \frac{\partial}{\partial y} \end{Bmatrix} = \frac{1}{\Delta} \begin{bmatrix} \sinh \eta \cos \phi & -\cosh \eta \sin \phi \\ \cosh \eta \sin \phi & \sinh \eta \cos \phi \end{bmatrix} \begin{Bmatrix} \frac{\partial}{\partial \eta} \\ \frac{\partial}{\partial \phi} \end{Bmatrix} \tag{A2}$$

where

$$\Delta = \sinh^2 \eta + \sin^2 \phi = \cosh^2 \eta - \cos^2 \phi$$
$$= \sinh^2 \eta \cos^2 \phi + \cosh^2 \eta \sin^2 \phi$$

Laplace's Equation

Laplace's equation is

$$\frac{\partial^2 \Phi}{\partial x^2} + \frac{\partial^2 \Phi}{\partial y^2} = \frac{1}{\Delta^2} \left(\frac{\partial^2 \Phi}{\partial \eta^2} + \frac{\partial^2 \Phi}{\partial \phi^2} \right) = 0 \tag{A3}$$

Through separation of variables, we obtain the fundamental solutions

$$1, \quad \phi, \quad \eta, \quad \eta\phi$$
$$e^{n\eta} \cos(n\phi), \qquad e^{n\eta} \sin(n\phi)$$
$$e^{-n\eta} \cos(n\phi), \qquad e^{-n\eta} \sin(n\phi)$$

When these solutions are used to represent pressure, the pressure must vanish at infinity and have discontinuities only on the airfoil. Thus, acceptable pressure functions are

$$\Phi_n = e^{-n\eta} \sin(n\phi) \quad n = 1, 2, 3, \ldots \tag{A4}$$

Due to the Δ^2 in the denominator of Eq. (A3), we must also

consider derived potential functions that have singularities at $\Delta = 0$ (leading and trailing edge of airfoil). We define symmetric and antisymmetric functions

$$\Phi_s = \sum_{n=1,3,5}^{\infty} 2\Phi_n = [\sin\phi \cosh\eta]/\Delta$$

(series converges $\eta \neq 0$)

$$\Phi_a = \sum_{n=2,4,6}^{\infty} (-2)\Phi_n = -[\sin\phi \cos\phi]/\Delta$$

(series converges $\eta \neq 0$) (A5)

We also define $\bar{\Phi}_1 \equiv \Phi_1 - \frac{1}{2}\Phi_s$, which yields zero net pressure across the airfoil.

Velocity Potentials

We also define a set of velocity potentials based on

$$\Psi_n = \int_{-\infty}^{x} \Phi_n(\xi, y)\, d\xi \tag{A6}$$

$$\Psi_s = \pi - \phi = \sum_{n=1,3,5}^{\infty} 2\Psi_n \quad \text{(series converges everywhere)}$$

$$\Psi_a = e^{-\eta}\sin\phi = \sum_{n=2,4,6}^{\infty} -2\Psi_n$$

(series converges everywhere)

$$\Psi_1 = \frac{1}{4}\Phi_2 + \frac{1}{2}\Psi_s = \bar{\Psi}_1 + \frac{1}{2}\Psi_s$$

$$\Psi_n = \frac{1}{2}\left(\frac{\Phi_{n+1}}{n+1} - \frac{\Phi_{n-1}}{n-1}\right) \qquad (n = 2, 3, 4, \ldots)$$

$$\Psi_a = \Phi_1, \qquad \bar{\Psi}_1 = \frac{1}{4}\Phi_2 \tag{A7}$$

On the airfoil ($\eta = 0$)

$$\hat{\Psi}_s = \sum_{n=1,2,3,4}^{\infty} 2\hat{\Phi}_n \qquad (\phi \neq 0) \tag{A8}$$

Gradients of Potentials

Let $(\,)' \equiv -\mathrm{d}(\,)/\mathrm{d}y$. This gives Φ_n' as the normal acceleration and Ψ_n' the normal velocity:

$$\Phi_s' = \sinh\eta\cosh\eta[(\cosh^2\eta + \cos^2\phi)\sin^2\phi + (\sin^2\phi - \sinh^2\eta)\cos^2\phi]/\Delta^3$$

$$\Phi_a' = \sinh\eta\cos\phi[\sinh^2\eta\cos^2\phi - 3\cosh^2\eta\sin^2\phi]/\Delta^3$$

$$\Phi_n' = ne^{-n\eta}[\cosh\eta\sin\phi\sin(\eta\phi) - \sinh\eta\cos\phi\cos(\eta\phi)]/\Delta \tag{A9}$$

$$\Psi_s' = \sinh\eta\cos\phi/\Delta$$

$$\Psi_a' = \Phi_1', \qquad \Psi_1' = \frac{1}{4}\Phi_2' + \frac{1}{2}\Psi_s'$$

$$\Psi_n' = \frac{1}{2}\left[\frac{\Phi_{n+1}'}{n+1} - \frac{\Phi_{n-1}'}{n-1}\right] \qquad (n = 2, 3, 4, \ldots) \tag{A10}$$

Appendix B: Acceleration Potential

In Eq. (11), Φ^V is expanded in a Φ_j series for the static case, in order to find the induced flow due to bound vorticity. If we expand this concept, we can develop differential equations for w_j based on Eq. (3a):

$$\Phi^V = -\sum \tau_j^V\Phi_j, \quad \Phi^A = -\sum \tau_j^A\Phi_j, \quad \Phi = -\sum \tau_j\Phi_j$$
$$w = \sum w_j\Psi_j', \quad \tau_j^A + \tau_j^V = \tau_j \tag{B1}$$

It follows from Eqs. (4) and (5) that $w_j = \tau_j^V$, and that

$$\dot{w} = \sum \dot{w}_j\Psi_j' = \sum (\tau_j - w_j)\Phi_j' \tag{B2}$$

The nature of the acceleration potential method is that the pressure (or velocity) expansions should balance on the airfoil. The Φ', Ψ' relationships in Appendix A show that Eq. (B2) is balanced when

$$\dot{w}_a - \tfrac{1}{2}\dot{w}_2 + w_1 = \tau_1$$
$$(1/2n)(\dot{w}_{n-1} - \dot{w}_{n+1}) + w_n = \tau_n \quad n = 2, 3, \ldots \tag{B3}$$

This is identical to the result from our thin-airfoil derivation, Eq. (23). However, the above equations are not complete since they omit the distributions w_s and w_a. The singularities associated with the derived functions Φ_s, Φ_a, Ψ_s' imply that the theory must be extended to include these singularities in order to obtain w_s, w_a equations. For the special case of no-shed vorticity ($\bar{\Gamma} = \gamma_s + \frac{1}{2}\gamma_1 = 0 \rightarrow w_s + \frac{1}{2}w_1 = 0$, $\lambda_j = 0$), the Ψ_s' terms disappear; and $w_a = \tau_a$, $w_s = \tau_s$ become the two extra equations. These cause the velocity balance to be fulfilled everywhere in the flowfield. These, then, agree with thin-airfoil theory ($\gamma_j = w_j$), Eq. (15a).

For the general case, the equation cannot be balanced everywhere; and the far field must become a "natural" boundary condition. The balance of $1/\sinh^3\eta$ leading-edge singularities gives

$$(\tau_s - w_s) = -(\tau_a - w_a) \quad \text{or} \quad w_s + w_a = \tau_s + \tau_a \tag{B4}$$

In other words, the classical thin-airfoil pressure distribution gives the classical inflow. (This is also equivalent to $\lambda_a = -\lambda_s$, which implies no leading-edge singularity due to shed vorticity.) The balance of $1/\sinh\eta$ singularities gives a second equation

$$\frac{2Z}{(1+Z)^2}(\tau_a - w_a) - \sum_n (-1)^{n-1}nZ^n(\tau_n - w_n) - (\dot{w}_s + \dot{w}_a) = 0 \tag{B5}$$

where $Z \equiv e^{-\eta}$. At $\eta = 0$, $Z = 1$, this gives

$$\frac{1}{2}(\tau_a - w_a) - \sum_n (-1)^{n-1}n(\tau_n - w_n) + (\dot{w}_s + \dot{w}_a) = 0 \tag{B6}$$

a divergent (although functionally correct) series. To manipulate this into a better-behaved series, we divide by Z and integrate from 0 to 1. The result is

$$\frac{2}{1+Z}(\tau_a - w_a) - \sum_n (-1)^{n-1}Z(\tau_n - w_n) - \sum_n \frac{b_n}{n}(\dot{w}_s + \dot{w}_a) = 0 \tag{B7}$$

where $\nu(0)$ is approximated by $-\Sigma\, b_n/n$ (Appendix C). This series still fails to converge at $Z = 1$, $(1 = 2 - 2 + 2 - 2 + 2 - 2 \ldots)$. However, when the diverging series of 2 is

replaced by a series of b_n (Appendix C), we have a well-behaved model:

$$(\tau_a - w_a) = \frac{1}{2}\sum_n b_n \left[(\tau_n - w_n) - \frac{2}{n}(\dot{w}_s + \dot{w}_a)\right] \quad \text{(B8)}$$

As a special case, consider no inflow due to bound vorticity: $\tau_a = 0$, $\tau_n = (2/n)\dot{\tau}_s$, Eqs. (15). The term $\dot{w}_s + \dot{w}_a = \dot{\tau}_s + \dot{\tau}_a = \dot{\tau}_s$ cancels every $b_n\tau_n$ term yielding

$$w_a = \frac{1}{2}\sum_n b_n w_n \qquad (w_j \equiv \lambda_j) \quad \text{(B9)}$$

This is the same as from the vorticity equations, Eq. (28). Also note that the $\dot{w}_s + \dot{w}_a$ coefficient, $\Sigma\, b_n/n$, approaches ∞, $-\chi_a(0)$, as N becomes large.

Appendix C: Shed-Wake Expansion

Consider the approximate expansion

$$1 \approx \sum_{n=1}^{N} b_n Z^n, \qquad 0 < Z \le 1 \quad \text{(C1)}$$

If we divide by Z and integrate from 0 to 1, we have

$$\chi_a(Z) - \chi_a(0) \approx \sum_{n=1}^{N} \frac{b_n}{n} Z^n \quad \text{(C2)}$$

Evaluation at $Z = 1$ yields the following:

$$1 = \sum_{n=1}^{N} b_n, \qquad -\chi_a(0) \approx \sum_{n=1}^{N} b_n/n \quad \text{(C3)}$$

Thus, $\Sigma\, b_n/n$ will approach ∞ as N is increased.

To apply a weighted least-squares calculation of b_n, we minimize J, where

$$J = \int_0^1 \left[1 - \sum b_n Z^n\right]^2 Y(Z)\, dZ \quad \text{(C4)}$$

$Y(Z)$ is a weighting function. Different weights will result in different inflow theories. For $Y(Z) = Z^z$ ($Z = 1$ is the most important point), we obtain an expansion

$$1 \approx 1 - (1 - Z)^N \quad \text{(C5)}$$

this further implies

$$b_n = (-1)^{n-1}\frac{n!}{N!(N-n)!}, \qquad \sum n b_n = 0 \quad \text{(C6)}$$

These are the binomial expansion coefficients of $(1 - Z)^N$.

For $Y(Z) = Z^q$, q = integer, we have a family of b_n. The case $q = -1$ (smallest possible integer value) gives a closed-form expression

$$b_n = (-1)^{n-1}\frac{(N+n)!}{(N-n)!}\frac{1}{(n!)^2} \quad \text{(C7)}$$

In this formulation, the $\Sigma\, b_n = 2$ for N odd, and $\Sigma\, b_n = 0$ for N even.

From Eq. (18) we see that the functional form of the λ_a, λ_n relationship is

$$\frac{1}{\sinh\eta} = \sum_{n=1}^{N} \frac{b_n e^{-n\eta}}{\sinh\eta} \quad \text{(C8)}$$

This shows that the error in the η functional involves a singularity at $\eta = 0$. Thus, for the least-square error from Eq. (C8) to be finite

$$\text{error} = \int_0^1 \left[1 - \sum b_n e^{-n\eta}\right]^2 \frac{1}{\sinh\eta}\, d\eta \quad \text{(C9)}$$

one must have $\Sigma\, b_n = 1$ in order to cancel the singularity. Thus, we also consider modifications of Eq. (C7) to meet this criterion. In particular, we define three possibilities: 1) modified least squares, b_N replaced by $b_N + (-1)^N$; 2) augmented least squares, b_n taken from formula for $N - 1$ terms and $b_N = (-1)^{N+1}$; and 3) least squares fit ($q = -1$) with formal constraint on $\Sigma\, b_n = 1$.

Acknowledgments

This work was sponsored by the U.S. Army Aeroflightdynamics Directorate (ATCOM), NASA Grant NAG-2-728, Robert A. Ormiston, Technical Monitor.

References

[1]Wagner, H., "Uber die Entstehung des dynamischen Auftriebs von Tragflugeln," ZAMM, Bd. 5, Heft 1, Feb. 1925, pp. 17–35.

[2]Theodorsen, T., "General Theory of Aerodynamic Instability and the Mechanism of Flutter," NACA Rept. 496, May 1934, pp. 413–433.

[3]Garrick, I. E., "On Some Reciprocal Relations in the Theory of Nonstationary Flows," NACA Rept. 629, 1938.

[4]Jones, R. T., "Operational Treatment of the Nonuniform Lift Theory to Airplane Dynamics," NACA TN 667, March 1938, pp. 347–350.

[5]Sears, W. R., "Operational Methods in the Theory of Airfoils in Non-Uniform Motion," *Journal of the Franklin Institute*, Vol. 230, July 1940, pp. 95–111.

[6]Jones, R. T., "The Unsteady Lift of a Wing of Finite Aspect Ratio," NACA Rept. 681, June 1939, pp. 31–38.

[7]Jones, W. P., "Aerodynamic Forces on Wings in Non-Uniform Motion," British Aeronautical Research Council, R & M 2117, Aug. 1945.

[8]Bisplinghoff, R. L., Ashley, H., and Halfman, R. L., *Aeroelasticity*, Addison–Wesley, Reading, MA, 1955.

[9]Edwards, J. W., Breakwell, J. V., and Bryson, A. E., Jr., "Reply by Authors to Vepa," *Journal of Guidance and Control*, Vol. 2, No. 5, 1989, pp. 447, 448.

[10]Hassig, H. J., "An Approximate True Damping Solution of the Flutter Equations by Determinant Iteration," *Journal of Aircraft*, Vol. 8, No. 11, 1971, pp. 825–889.

[11]Vepa, R., "On the Use of Padé Approximants to Represent Unsteady Aerodynamic Loads for Arbitrarily Small Motions of Wings," AIAA Paper 76-17, Jan. 1976.

[12]Dowell, E. H., "A Simple Method for Converting Frequency Domain Aerodynamics to the Time Domain," NASA TM-81844, Oct. 1980.

[13]Edwards, J. W., Ashley, H., and Breakwell, J. V., "Unsteady Aerodynamic Modeling for Arbitrary Motions," AIAA Paper 77-451, March 1977.

[14]Edwards, J. W., Breakwell, J. V., and Bryson, A. E., Jr., "Active Flutter Control Using Generalized Unsteady Aerodynamic Theory," *Journal of Guidance and Control*, Vol. 1, Jan.–Feb. 1978, pp. 32–40.

[15]Matsushita, H., "Aerodynamic Transfer Functions of a Finite Wing in Incompressible Flow," 20th Aircraft Symposium, Fukuoka, Japan, Nov. 1982.

[16]Miyazawa, Y., and Washizu, K., "A Finite State Aerodynamic Model for a Lifting Surface in Incompressible Flow," *AIAA Journal*, Vol. 21, No. 2, 1983, pp. 163–171.

[17]Loewy, R. G., "A Two-Dimensional Approximation to Unsteady Aerodynamics in Rotary Wings," *Journal of the Aeronautical Sciences*, Vol. 24, No. 2, 1957, pp. 81–92.

[18]Dinyavari, M. A. H., and Friedmann, P. P., "Unsteady Aerodynamics in Time and Frequency Domains for Finite Time Arbitrary Motion of Rotary Wings in Hover and Forward Flight," AIAA Paper 84-0988, May 1984.

[19]Beddoes, T. S., "Representation of Airfoil Behavior," *Vertica*, Vol. 7, No. 2, 1983, pp. 183–197.

[20]Tran, C. T., and Petot, D., "Semi-Empirical Model for Dynamic

Stall of Airfoils in View of the Application to the Calculation of Response of a Helicopter Blade in Forward Flight," Sixth European Rotorcraft and Powered Lift Forum, Bristol, England, UK, Sept. 1980.

[21]Peters, D. A., "Toward a Unified Lift Model for Use in Rotor Blade Stability Analyses," *Journal of the American Helicopter Society*, Vol. 30, No. 3, 1985, pp. 32–42.

[22]Peters, D. A., and Su, A., "An Integrated Airloads-Inflow Model for Use in Rotor Aeroelasticity and Control Analysis," *Mathematical and Computer Modelling*, Vol. 19, Nos. 3/4, 1994, pp. 109–123.

[23]Dowell, E. H., Curtiss, H. C., Jr., Scanlan, R. H., and Sisto, F., *A Modern Course in Aeroelasticity*, Sijthoff and Noordhoff, Alphen aan den Rijn, The Netherlands, 1980.

[24]Cicala, P., "Le Azioni Aerodinamiche sui Profili di ala Oscillanti in Prezenza di Corrente Uniforme," Memoirs of the Royal Academy of Science, Torino, Serie 2, Tomo 68, Parte I, July 7, 1935.